ELSEVIER

International Journal of Mass Spectrometry 190/191 (1999) 195–207

International Journal of Mass Spectrometry

Ion/molecule reactions of perfluorotributylamine (FC43) cations with polycyclic aromatic hydrocarbons in a quadrupole ion trap

Andrew A. Mosi, William R. Cullen, Günter K. Eigendorf*

Department of Chemistry, University of British Columbia, Vancouver, B.C. V6T 1Z1, Canada

Received 28 September 1999; accepted 9 February 1999

Abstract

Ion/molecule reactions between fluorocarbon cations, generated from perfluorotributylamine (FC43), and polycyclic aromatic hydrocarbons (PAHs) were carried out in a quadrupole ion trap by mass isolating individual types of FC43 ions (R^+) and reacting them with PAHs eluting from a GC column. The observed products resulting from these reactions consisted of $[M + R]^+$ adducts and $[M + R - nHF]^+$ ($n = 1,2$) elimination products. The relative abundance of these products was found to vary between different PAH structural isomers, such as anthracene and phenanthrene, thus enabling isomer differentiation. Of particular interest was the reactivity of the $C_3F_5^+$ cation because this species yielded the most abundant and diverse reaction chemistry. Formation of adducts versus molecular ions appears to be strongly influenced by the ionization energy (IE) of the PAHs. Using this ion/molecule reaction technique several PAH isomers, present in a PAH contaminated environmental sediment extract, could be identified. (Int J Mass Spectrom 190/191 (1999) 195–207) © 1999 Elsevier Science B.V.

Keywords: Ion/molecule reactions; Quadrupole ion trap; Perfluorotributylamine; Polycyclic aromatic hydrocarbons; Isomer differentiation

1. Introduction

Mass spectrometry has become an important tool in modern analytical chemistry because of its high sensitivity and ability to provide molecular structure information. However, the differentiation of structural isomers remains a challenging task, especially when using electron ionization (EI) to analyze substances that are present in complex mixtures, such as biological and environmental specimen. Isomeric compounds, such as linear or branched hydrocarbons, can often be distinguished by small differences in their source-produced fragmentation patterns. These might be due to specific substitution patterns, position of double bonds, or branching points that will initiate a specific fragmentation process. In such cases ion source conditions, such as temperature and ionization energy, have to be tightly controlled. Isomeric bio-organic substances, like the differences in amino acids sequence in peptides for instance, can generally be distinguished by in-source or post-source fragmentation patterns. Isomers of cyclic compounds, such as terpenes, are very difficult to differentiate unless a specific ring junction (α versus β) or substituent will initiate fragmentation preferentially. In such cases the fragmentation patterns of isomers are often very

* Corresponding author. E-mail: eigen@chem.ubc.ca

Dedicated to J.F.J. Todd and R.E. March in recognition of their original contributions to quadrupole ion trap mass spectrometry.

PII S1387-3806(99)00028-7

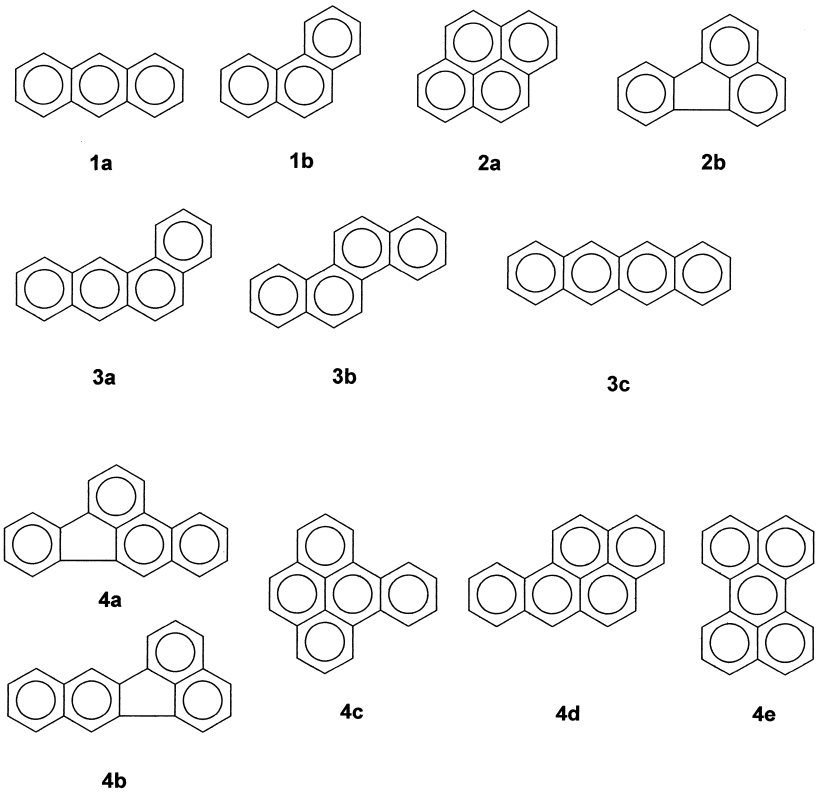

Fig. 1. PAH isomers investigated (anthracene **1a**, phenanthrene **1b**, pyrene **2a**, fluoranthene **2b**, benz[a]anthracene **3a**, chrysene **3b**, tetracene **3c**, benzo[b]fluoranthene **4a**, benzo[k]fluoranthene **4b**, benzo[e]pyrene **4c**, benzo[a]pyrene **4d**, perylene **4e**).

similar or even identical and only small differences can be observed in the relative abundance of some fragment ions. Isomeric substitution, such as in cyclic hydroxyl compounds, might lead to preferential elimination of neutral species (e.g. H_2O), again leading to virtually identical patterns and only slight differences in relative intensities. In general, structural isomers that yield identical EI spectra cannot be distinguished from each other unless chromatographic retention times can be employed for differentiation or NMR techniques are used, requiring larger amounts of analyte. One important class of compounds, whose isomers cannot be differentiated by EI mass spectrometry, are polycyclic aromatic hydrocarbons (PAHs). PAHs form a large class of chemical compounds, containing numerous isomeric species, that are dispersed into the environment from natural and anthropogenic sources [1]. PAH isomers, such as those outlined in Fig. 1, provide under EI conditions identical mass spectra. In addition to the highly stable molecular ions very little fragmentation is observed. However, since many PAHs have been identified as carcinogens and their toxicological properties are often isomer dependent [2], it is critical to be able to differentiate the various isomers, particularly in areas of environmental concern. Mass spectrometric isomer differentiation of PAHs has been carried out previously via ion/molecule reactions using chemical ionization (CI) conditions. Several CI techniques have been reported for PAH isomer differentiation using O_2/N_2 [3–7] and CO_2, [8,9] under negative CI conditions and dimethylether [10], dimethylsulfide [11], and diethylether [12] under positive CI conditions. However, because these methods were developed for high CI reagent gas pressures (0.1–1 Torr; 1 Torr = 133.3 Pa) they are not well suited for use in ion trap

mass spectrometers that operate at much lower reagent gas pressures (e.g. 10^{-5} Torr). For example, when dimethylether was used as a CI gas in an ion trap the results obtained at high pressure [10] could not be reproduced [13]. Similarly, reported negative chemical ionization techniques [3–9] cannot be attempted on some commercially available gas chromatography/mass spectrometry (GC/MS) ion trap instruments because they are often not equipped with conversion dynodes. More importantly though, the low pressure in an ion trap does not provide suitable conditions for production of sufficient amounts of negative ions [14]. However, because of their high sensitivity and ability to perform multiple MS/MS experiments, ion traps have become popular and relatively inexpensive alternatives to linear quadrupoles (which operate with standard high pressure CI sources) particularly for detection and identification of compounds present in very low concentrations, such as in environmental applications. The combination of chromatographic techniques [GC, high-performance liquid chromatography (HPLC)] with an ion trap has provided suitable means for sample introduction. The high sensitivity of an ion trap and its ability for selective mass storage [15] provides a facility for experiments previously accessible via Fourier transform ion cyclotron resonance (FTICR) instruments of much higher costs only. As mentioned earlier, many of the previously reported CI experiments cannot be reproduced in an ion trap. However, the high sensitivity of this instrument led us to attempt other CI methods for differentiating PAH isomers. For instance, we found that halogenated hydrocarbons, such as 1,1-difluoroethane, proved to be suitable reagents for generating isomer specific mass spectra [16,17]. These reagents form adducts of the type $[M + R]^+$ and $[M + R - HX]^+$ (M = PAH, R = reagent gas ion, X = CI or F). Differences in the relative amounts of these adducts with respect to M^+ and MH^+ as well as formation of specific adducts, enabled differentiation of PAH isomers. These results suggested that other hydrocarbon ions of the type $C_aH_bX_c^+$ (X = CI, F) are likely to form adducts with PAHs. It was found that adduct formation was dependent on the ionization energies (IE) of the PAH and halocarbon cations. In these studies it was also noticed that fluorine containing compounds led to higher yields of adducts. This prompted us to investigate Perfluorotributylamine $(C_4F_9)_3N$, commonly referred to as FC43, as a CI reagent. Under EI conditions it yields numerous ions of the type $C_nF_m^+$ and $C_nF_mN^+$ (n = 1–12, m = 1–24) that are often used as mass calibration markers in mass spectrometry. In consideration of our previous results [16,17] and the reported reactivity of CF_3^+ towards aromatic compounds [18–21] we thought that these ions should provide a series of possible reagents for adduct formation with PAHs. In this article we report on the reactions between a number of mass selected FC43 ions and isomeric PAHs using a quadrupole ion trap.

2. Experimental

2.1. Standards and reagents

The PAHs anthracene **1a**, phenanthrene **1b**, pyrene **2a**, fluoranthene **2b**, benz[a]anthracene **3a**, chrysene **3b**, benzo[b]fluoranthene **4a**, benzo[k]fluoranthene **4b**, and benzo[a]pyrene **4d** were obtained from a standard 2000 μg mL^{-1} solution purchased from Supelco (Oakville, Ontario, Canada) and diluted with toluene to give a 50 μg mL^{-1} (each) solution. Solutions (50 μg mL^{-1}) of tetracene **3c**, benzo[e]pyrene **4c**, and perylene **4e** were prepared from pure compounds obtained from Aldrich (Milwaukee, WI).

FC43 (Varian, Walnut Creek, CA) was introduced into the ion trap through a needle valve.

2.2. Instrumentation

All experiments were performed on a Saturn 4D GC/MS/MS system (Varian, Walnut Creek, CA) equipped with a Wave-Board for the generation of user-defined waveforms for application to the ion-trap electrodes. This trap could only be operated in positive ion mode. Thus, all results reported here refer to positive ions only. The trap temperature was maintained at 255 °C. The FC43 introduced into the trap was ionized with an electron beam of 70 eV. The multiplier voltage was optimized to give a gain of 10^5.

Vacuum conditions were monitored via intensity of the background spectrum (air, water) because this instrument is not equipped with a vacuum gauge.

2.3. Procedure

PAH samples were introduced into the ion trap from a gas chromatograph using a DB5 capillary column [30 m × 0.25 mm inner diameter (i.d.)], 0.25 μm film thickness) from J & W (Folsom, CA), that was inserted directly into the trap through a transfer line maintained at 280–290 °C. Samples were introduced via splitless injection at 290 °C. The GC column temperature program consisted of a 90 °C initial temperature for 0.1 min followed by a 6 °C min^{-1} ramp to 280 °C, holding at 280 °C for 1 min and then ramping to 300 °C at 20 °C min^{-1} and holding for 20 min. Helium gas was used as a carrier at a linear velocity of 32 cm s^{-1}, corresponding to a flow of ~1 mL min^{-1} into the ion trap. Details on the use of the Saturn ion trap for chemical ionization have been reported previously [16]. The most important trap parameters employed in this work were: emission current 10 μA, ionization storage level (ISL) of *m/z* 35, reaction storage level (RSL) of *m/z* 35, background storage level (after the reaction period) of *m/z* 35, ionization time (IT) of 500 μs and reaction time (RT) of 100–128 ms. The automatic reaction control (ARC) function for constantly optimizing the RT and IT values in the CI scan function was not used because the ion/molecule reactions took place during the MS/MS scan function. Consequently, these experiments were all carried out under constant IT and RT conditions.

Isolation of individual ions was achieved by using the standard MS/MS isolation function available via the SATURN version 5.2 software. By keeping the collision induced dissociation (CID) energy at 0 V mass isolation with a 1 u window was achieved without fragmentation. The CI reaction time value was kept at 1 ms (minimum value) because the reaction time between isolated ions and analyte molecules will depend upon the CID time value in the MS/MS function. Unless otherwise indicated, a CID time of 100 ms was used. In order to generate sufficient reagent ions, the ionization time for the single mass ion isolation experiments was increased to 1000–2500 μs.

Table 1
Ions generated from the EI of FC43 and their MS/MS isolation efficiency; % RI = relative intensity

m/z	Assigned formula	EI ionization counts (% RI)	MS/MS isolation counts (% RI)	MS/MS mass-isolation efficiency
69	CF_3^+	291 000 (100)	4000 (100)	1.4
93	$C_3F_3^+$	6900 (2)	100 (3)	1.4
100	$C_2F_4^+$	59 000 (20)	600 (15)	1.0
114	$C_2F_4N^+$	22 000 (7)	200 (5)	0.9
119	$C_2F_5^+$	34 000 (12)	40 (1)	0.1
131	$C_3F_5^+$	243 000 (84)	2000 (50)	0.8
150	$C_3F_6^+$	7000 (2)	60 (2)	0.8
164	$C_3F_6N^+$	5700 (2)	50 (1)	0.9
169	$C_3F_7^+$	11 000 (4)	10 (0.3)	0.1
181	$C_4F_7^+$	18 000 (6)	100 (3)	0.6
219	$C_4F_9^+$	49 000 (17)	0 (0)	0
264	$C_5F_{10}N^+$	58 000 (20)	100 (3)	0.2
314	$C_6F_{12}N^+$	3900 (1)	0 (0)	0
364	$C_7F_{14}N^+$	4700 (2)	0 (0)	0
414	$C_8F_{16}N^+$	26 000 (9)	20 (1)	0.1
426	$C_9F_{16}N^+$	5000 (2)	10 (0.3)	0.2
464	$C_9F_{18}N^+$	10 000 (3)	0 (0)	0
502	$C_9F_{20}N^+$	8000 (3)	0 (0)	0
614	$C_{12}F_{24}N^+$	9500 (3)	0 (0)	0

4. Results and discussion

The major ions formed during EI of FC43 in an ion trap are shown in Table 1, together with their relative abundance values and mass isolation efficiency. The PAHs analyzed in this work are shown in Fig. 1. Initially, FC43 was tested as a CI reagent gas by allowing all of its ions (Table 1) to react simultaneously with anthracene **1a** and phenanthrene **1b** eluting from the GC column. The resulting mass spectra are shown in Fig. 2(a). Both look very similar except for small amounts of adducts in the spectrum for **1b** (e.g. *m/z* 227). Formation of $M^{+\cdot}$ (*m/z* 178) generated by charge exchange appears to be the dominant process, together with $[M + 1]^+$ and some fragmentation products ($[M - H]^+$, $[M - 2H]^+$ and $[M - C_2H_2]^+$). A significant portion of the [M +

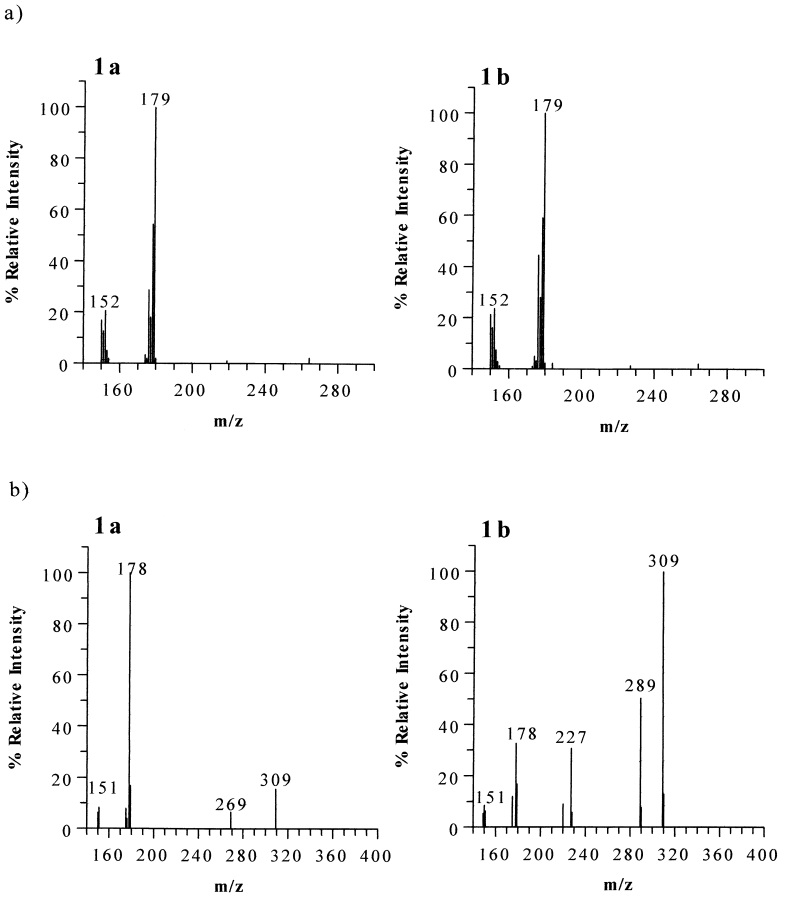

Fig. 2. (a) FC43 chemical ionization mass spectra of anthracene **1a** and phenanthrene **1b** (b) $C_3F_5^+$ ion/molecule reaction spectra of anthracene **1a** and phenanthrene **1b**.

$1]^+$ must arise from formation of MH^+ because ^{13}C contribution is only ~15%. Because FC43 lacks any protons, MH^+ could be formed via proton abstraction from $M^{+\cdot}$ ions or from residual proton sources in the ion source (H_2O). The lack of significant amounts of adduct ions, a requirement for isomer differentiation, would suggest that FC43 is not a useful reagent for PAHs when all of its ions are reacted simultaneously. Furthermore, the presence of all reagent ions could result in a high background, limiting the sensitivity of the analysis. Thus, PAHs reactions were investigated with individually mass-selected FC43 ions. Many of these experiments yielded interesting mass spectra. For example, when the *m/z* 131 ($C_3F_5^+$) ion was isolated and allowed to react with PAHs **1a** and **1b**, a number of intense adducts were obtained from both compounds [Fig. 2(b)]. The largest number of adducts were formed by **1b** (*m/z* 227 = [M + 49], *m/z* 289 = [M + 111] and *m/z* 309 = [M + 131]). Isomer **1a** reacted differently with $C_3F_5^+$ forming *m/z* 309 ions but at a significantly lower relative intensity, not yielding any *m/z* 289 or *m/z* 227 ions but forming a *m/z* 269 = [M + 91] product not observed with **1b**. Comparison of the two spectra reveals that these two structural isomers can be clearly distinguished from each other using $C_3F_5^+$ as a reagent ion. The [M + 111] and [M + 91] adducts correspond to successive losses of HF from the [M + 131] = $[M + C_3F_5]^+$ adduct while [M + 49] is due to $[M + C_3F_5 - C_2F_3H]^+$. Loss of HF from a fluorocarbon/PAH

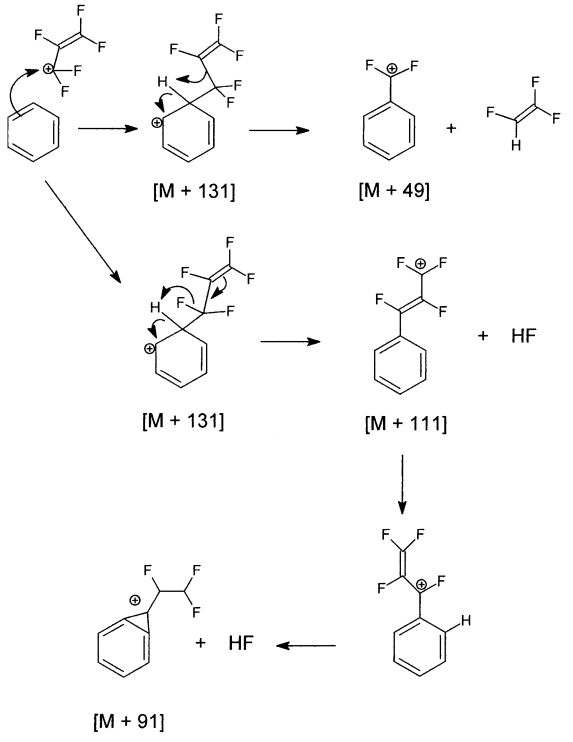

Fig. 3. Proposed mechanism for the formation of $[M + 131]^+$, $[M + 111]^+$, $[M + 91]^+$, and $[M + 49]^+$ ions from the reaction of $C_3F_5^+$ with a PAH molecule.

adduct has been observed previously, and was shown to include loss of H from the PAH skeleton [16]. A possible mechanism for the formation of these ions is illustrated in Fig. 3. Loss of HF and C_2F_3H moieties suggests that the [M + 131] adduct is a covalently bound species formed via an electrophilic attack rather than a weakly bound electrostatic complex. Compound **1b** again displays evidence of MH^+ formation based upon the relatively high [M + 1]/M ratio exceeding $^{13}C/^{12}C$.

The effect of analyte concentration on the distribution of product ions, during ion/molecule reactions with $C_3F_5^+$, was investigated by analyzing the mass spectra generated along the GC elution profile of compounds **1a** and **1b**. A relative measure of an increase in analyte concentration is given by increasing RIC (reconstructed ion count = sum of all ions) values. Fig. 4 summarizes the results for the main ions of interest. For both compounds no significant changes are noted in the relative ion counts (counts/RIC) at higher concentrations (i.e. RIC $>$ 2000). It is only in the lower concentration region (RIC $<$ 2000) that variations can be noted. For **1a**, only $M^{+\cdot}$ formed at low concentrations, possibly indicating a limiting ratio of analyte versus reagent ions for adduct formation to occur. On the other hand **1b** displayed significant adduct formation (*m/z* 289, *m/z* 309) at low concentrations with no $M^{+\cdot}$ formation, indicating a preferential reactivity of this compound with $C_3F_5^+$ reflecting the results seen for **1b** in Fig. 2(b).

Although Fig. 4 shows some variability in the relative intensity of the ions as a function of concentration, the ratio of ion counts between different mass ions remains relatively constant. For example, the average *m/z* 309/289 ratio of **1b** over the concentration range shown in Fig. 4 is 1.8 ± 0.2 [at a 90% confidence level (CL)]. Similarly, for **1a** the average *m/z* 178/309 ratio is 5.0 ± 0.6 (90% CL). Consequently, isomers can be clearly distinguished based upon their relative ratios of adduct versus molecular ions even when their percent relative intensity (RI) values vary due to changes in analyte concentration.

Another factor to be investigated was the time that $C_3F_5^+$ ions would be interacting with the PAH compound. This is summarized in Table 2. Increasing the reaction time resulted in a decrease in the relative amounts of $M^{+\cdot}$ observed for both compounds and an increase in the abundance of $[M + C_3F_5]^+$ ions. Again, this effect was much more pronounced for **1b**. The increased abundance of the $[M + C_3F_5]^+$ adducts at longer reaction times may be a result of greater collisional stabilization, particularly since their increase in abundance is not accompanied by a comparable increase in the abundance of the elimination products $[M + C_3F_5 - HF]$ (*m/z* 289) and $[M + C_3F_5 - 2HF]$ (*m/z* 269).

In addition to $C_3F_5^+$, other ions of FC43 were individually mass selected and reacted with PAHs **1a** and **1b**. The results from these ion/molecule reactions are summarized in Table 3. These data illustrate that the ions undergoing the largest amount of adduct formation are *m/z* 69 (CF_3^+), 93 ($C_3F_3^+$), 114 ($C_2F_4N^+$), and 131 ($C_3F_5^+$). For these four reagent ions, distinct differences can be seen in the adduct

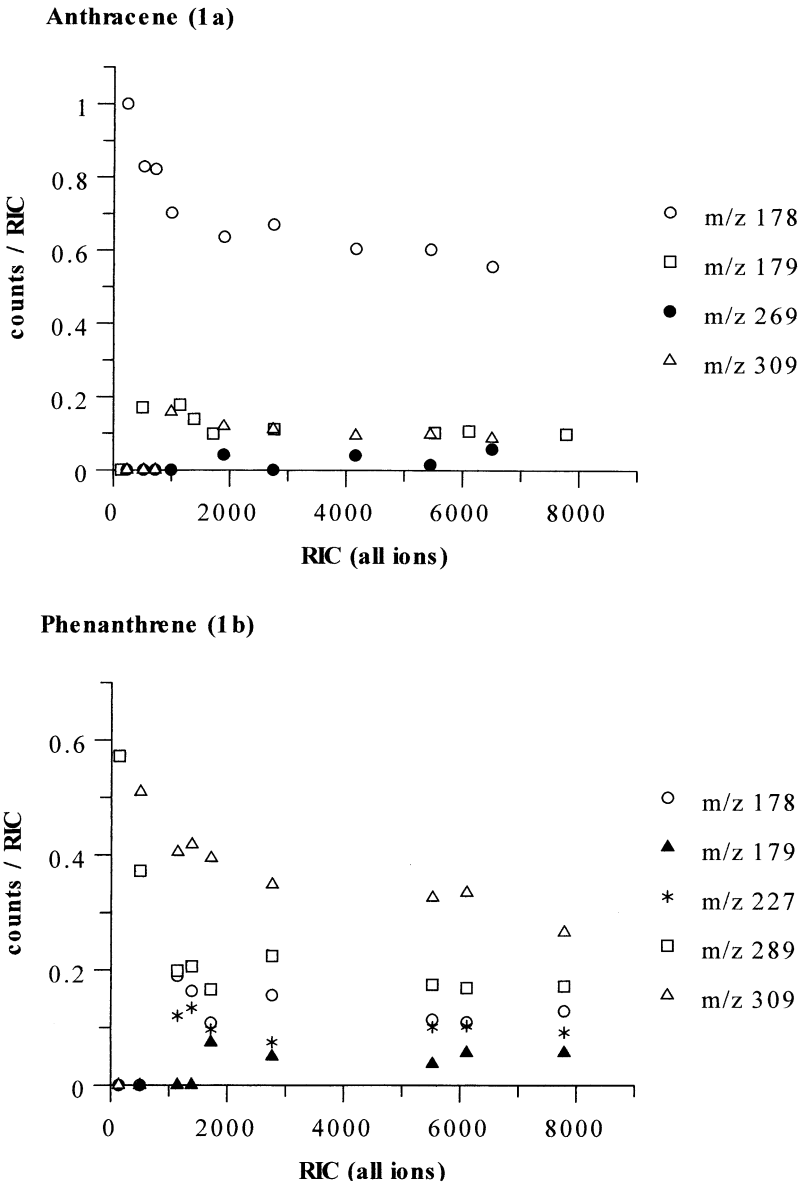

Fig. 4. Effect of analyte concentration on the relative abundance of ions produced with $C_3F_5^+$ for (upper) anthracene (**1a**) and (lower) phenanthrene (**1b**).

formations with compounds **1a** and **1b**. The reaction behavior of reagent ions *m/z* 69 and 93 ions is similar to the effects observed for halocarbon ions investigated previously [16], where compound **1b** was shown to form a greater abundance of the elimination product $[M + R - HF]^+$ with respect to addition product $[M + R]^+$. Conversely, **1a** yielded less or no $[M + R - HF]^+$ product but formed the $[M + R]^+$ adduct [16]. With $R = C_3F_5^+$ (*m/z* 131) **1b** reacts to produce a larger abundance of $[M + R]^+$ than $[M + R - HF]^+$. Elimination of HF is probably a good stabilization mechanism for energized $[M + R]^{+*}$ ions that have not undergone collisional or radiative stabilization. The data for the reaction products ob-

Table 2
Relative ratio of ions produced from $C_3F_5^+$ + PAH **1a** or **1b** normalized to total ion count at different reaction times (CID time)

CID Time (ms)	Anthracene (**1a**) (counts/Σ counts)			Phenanthrene (**1b**) (counts/Σ counts)			
	m/z 178	*m/z* 269	*m/z* 309	*m/z* 178	*m/z* 227	*m/z* 289	*m/z* 309
1	0.90	0.06	0.05	0.40	0.10	0.18	0.14
10	0.83	0.06	0.10	0.25	0.13	0.23	0.34
100	0.79	0.06	0.15	0.14	0.13	0.29	0.41

tained when using a variety of different fluorinated and chlorinated reagent ions are summarized in Table 4 together with the data for the CF_3^+ and $C_3F_5^+$ FC43 ions. As seen from Table 4, **1b** yields a greater $[M + R - HX]^+/[M + R]^+$ ratio than **1a**, with a variety of halocarbon ions, indicating that a greater proportion of the formed $[M + R]^+$ ions have to be stabilized by elimination of HX. The necessity of **1b** $[M + R]^+$ adducts to be stabilized is probably a result of larger electrostatic attraction between **1b** and R^+ stemming from the higher polarizability of **1b** versus **1a** (polarizability constants $\alpha = 38.8 \times 10^{-24}$ cm^3 for **1b** and $\alpha = 25.4 \times 10^{-24}$ cm^3 for **1a**) [22]. The unusually high yield of $[M + C_3F_5]^+$ for **1b** indicates that this adduct must be more stable than those with other halocarbon ions.

The reactivity of the CF_3^+ and $C_3F_5^+$ ions was investigated further by reacting them successively with PAHs **1a**–**4e**. The data in Tables 5 and 6 show that PAHs with low IE values yield lower abundance of adducts. Our previous work [16] has shown that for isomeric compounds such as **1a** and **1b**, the preferred formation of the $[M + R - HF]^+$ elimination product is associated with the higher IE PAH species (IE > 7.5 eV). By comparing the total ion counts of ion species (e.g. M^+) normalized to the sum of all the major ions, to the PAHs ionization energy, it was possible to observe some significant trends. Tables 7 and 8 represent the linear regression data from ion/molecule reactions with CF_3^+ and $C_3F_5^+$, respectively. Both CF_3^+ and $C_3F_5^+$ display an increase in the abundance of PAH molecular ion formation at lower IE. Such a trend is expected as charge exchange becomes more favored; this has been observed previously with other halocarbon ions [16,17]. An opposite trend occurs when the normalized sum of all the major adduct ions (i.e. sum of adduct ions/sum of all ions) is compared to IE data. Higher IE values lead to a greater abundance of ionization via adduct formation because charge exchange is less energetically favorable. For the ion/molecule reaction with $C_3F_5^+$ this trend is dominated by the formation of [M + 131]

Table 3
Mass spectral data (% RI) for ion/molecule reactions between individually mass selected FC43 ions and PAHs **1a** and **1b**

	M = Anthracene (**1a**)					M = Phenanthrene (**1b**)				
R^+	[M]	[M + 1]	[M + R]	[M + R − HF]	[M + R − 2HF]	[M]	[M + 1]	[M + R]	[M + R − HF]	[M + R − 2HF]
69	100	15	5	5	0	100	30	10	80	10
93	100	20	10	20	0	70	10	0	100	0
100	100	15	0	0	0	100	10	0	0	0
114	100	10	50	0	0	5	0	0	0	0
119	100	20	0	0	0	100	15	5	1	0
131	100	15	15	0	10	50	15	100	60	0
150	100	0	0	0	0	100	0	0	0	0
164	0	0	0	0	0	0	0	0	0	0
169	0	0	0	0	0	0	0	0	0	0
181	100	0	0	0	0	100	0	0	0	0
264	100	15	20	0	0	100	20	0	0	0
414	100	30	0	0	0	100	0	0	0	0

Table 4
Mass spectral data (% RI) for ion/molecule reactions between individually mass selected halocarbon ions and PAHs **1a** and **1b**

R^+	[M]	[M + 1]	[M + R]	[M + R − HX]	[M + R − 2HX]	[M + R − HX]/[M + R]
M = Anthracene (**1a**)						
$CHCI_2^+$	100	16	0.5	2	0	4
CCI_3^+	100	15	0.5	0	0	0
CF_3^+	100	15	6	5	0	0.8
$CH_3CF_2^+$	100	45	55	11	0	0.2
$C_2H_4CI^+$	100	16	20	3	N.A.	0.15
$C_3H_6CI^+$	100	38	30	10	N.A.	0.3
$C_3F_5^+$	100	15	15	0	10	0
M = Phenanthrene (**1b**)						
$CHCI_2^+$	100	16	0	52	0	large
CCI_3^+	100	16	2	13	0	7
CF_3^+	100	19	11	85	12	7.7
$CH_3CF_2^+$	35	100	13	100	0	7.7
$C_2H_4CI^+$	100	20	4	22	N.A.	6
$C_3H_6CI^+$	100	65	13	15	N.A.	1.1
$C_3F_5^+$	50	15	100	60	0	0.6

ions, as illustrated by the positive correlation between the [M + 131] relative ion counts and IE of the PAHs (slope = +0.64, r = 0.89). On the other hand, the CF_3^+ data illustrate that the elimination products are important reaction channels because the [M + 69] ion data do not correlate (r = 0.27) with IE on their own.

In general, PAHs with higher IE values result in less charge exchange products yielding more adduct formation. This trend is expected to be most significant when the IE of the reagent ions is close to or lower than the IE of the PAH. In such instances charge exchange may not take place, or it will be a minor reaction pathway. For example, the IE of $CH_3CF_2^+$ is 7.92 eV [23], is close to that of **1b**. As illustrated in Table 4, the molecular ion is not the base peak in the reaction spectrum between $CH_3CF_2^+$ and **1b**. The IE of CF_3 is 9.5 eV [23] and, as expected, $M^{+\cdot}$ is the base peak in the reaction spectra of all the

Table 5
Mass spectral data (% RI) for the reaction between CF_3^+ (*m/z* 69) and PAHs **1a** to **4e**

PAH	Mr (u)	IE (eV)[a]	[M] M^+	[M + 1]	[M + 29] $[M + R - 2HF]^+$	[M + 49] $[M + R - 2HF]^+$	[M + 69] $[M + R]^+$
Anthracene (**1a**)	178	7.45	100	15	0	5	5
Phenanthrene (**1b**)	178	7.9	100	30	10	80	10
Pyrene (**2a**)	202	7.43	100	17	0	8	10
Fluoranthene (**2b**)	202	7.95	100	18	0	65	88
Benz[a]anthracene (**3a**)	228	7.48	100	18	1	4	18
Chrysene (**3b**)	228	7.6	100	19	4	15	30
Tetracene (**3c**)	228	6.97	100	15	0	0	13
Benzo[b]fluoranthene (**4a**)	252	7.9[b]	100	25	0	33	63
Benzo[k]fluoranthene (**4b**)	252	7.4[b]	100	22	0	8	38
Benzo[e]pyrene (**4c**)	252	7.43	100	30	0	7	35
Benzo[a]pyrene (**4d**)	252	7.12	100	18	0	1	12
Perylene (**4e**)	252	6.95	100	24	0	0	0

[a] IE energy values obtained from Lias [23].
[b] Calculated using Huckel molecular orbital theory.

Table 6
Mass spectral data (% RI) for the reaction between $C_3F_5^+$ (*m/z* 131) and PAHs **1a** to **4e**

PAH	Mr (u)	IE (eV)[a]	[M] M^+	[M + 1]	[M + 49]	[M + 91] $[M + R - 2HF]^+$	[M + 111] $[M + R - HF]^+$	[M + 131] $[M + R]^+$
Anthracene (**1a**)	178	7.45	100	20	0	10	0	15
Phenanthrene (**1b**)	178	7.9	30	20	30	0	50	100
Pyrene (**2a**)	202	7.43	100	20	0	0	0	25
Fluoranthene (**2b**)	202	7.95	25	5	15	4	7	100
Benz[a]anthracene (**3a**)	228	7.48	100	30	0	0	0	40
Chrysene (**3b**)	228	7.6	80	25	5	0	4	100
Tetracene (**3c**)	228	6.97	100	20	0	0	0	0
Benzo[b]fluoranthene (**4a**)	252	7.9[b]	40	15	5	0	0	100
Benzo[k]fluoranthene (**4b**)	252	7.4[b]	90	35	0	0	0	100
Benzo[e]pyrene (**4c**)	252	7.43	100	25	0	0	0	60
Benzo[a]pyrene (**4d**)	252	7.12	100	35	0	0	0	20
Perylene (**4e**)	252	6.95	100	35	0	0	0	0

[a] IE energy values obtained from Lias [23].
[b] Calculated using Huckel molecular orbital theory.

PAHs analyzed (Table 5). The IE for $C_3F_5^+$ is not available, but the data in Table 6 indicate that it is probably close to or lower than 7.9 eV because reaction with **1b**, **2b**, and **3a** (PAHs with IE values close to 7.9 eV) yielded low abundance of $M^{+\cdot}$ and large amounts of ion/molecule reaction products.

The data in Tables 5 and 6 also demonstrate that isomers in the four PAH groups display significant differences in their CF_3^+ and $C_3F_5^+$ ion/molecule reaction spectra. Thus, these ion/molecule reactions provide a means to differentiate the structural isomers from each other in each PAH group. Other FC 43 ions, such as *m/z* 93 and 114, yielded similar results when reacted with these four groups of PAH isomers.

To test the viability of these ion/molecule reactions for performing isomer differentiation, an environmental sample consisting of a PAH contaminated sediment extract, was analyzed using $C_3F_5^+$ (*m/z* 131) as reagent. Fig. 5 shows the M, [M + 49], [M + 91], [M + 111], and [M + 131] extracted ion chromatograms for the PAHs **1a** and **1b** along with their monomethyl analogues. A comparison of the ion chromatograms clearly reveals that differences in relative intensities could be used to differentiate between the anthracene (**1a**) and phenanthrene (**1b**) compounds. This is confirmed by comparing the extracted mass spectra at positions 1 and 2, which show the presence of anthracene and phenanthrene, respectively. Mass spectra extracted at positions 3 and 4 identify respective mono methyl isomers (Fig. 6). These differences can be enhanced by performing simple mathematical transformations [17] on some of the ion chromatograms. For example, taking the difference between the normalized [M + 131] and M

Table 7
Summary of the linear regression parameters describing the relationship between the relative intensities of the products from CF_3^+ + PAH ion/molecule reaction and the ionization energy (eV) of the PAHs

Ions[a,b]	Slope (1/eV)	Std. dev. (1/eV)	Intercept[c]	Std. dev.	Correlation coefficient (*r*)
M^+	−0.40	0.05	3.6	0.4	−0.90
$[M + 69]^+$	0.060	0.057	−0.33	0.44	0.27
$[M + 69]^+ + [M + 49]^+ + [M + 29]^+$	0.46	0.06	−3.2	0.5	0.89

[a] Ion counts have been normalized by dividing by the summed intensity of all the major ions observed.
[b] These results are for the PAHs listed in Table 5 and 6.
[c] Unitless because relative ion counts are unitless.

Table 8
Summary of the linear regression parameters describing the relationship between the relative intensities of the products from $C_3F_5^+$ + PAH ion/molecule reaction and the ionization energy (eV) of the PAH

Ions[a,b]	Slope (1/eV)	Std. dev. (1/eV)	Intercept[c]	Std. dev.	Correlation coefficient (r)
M^+	−0.59	0.08	4.9	0.6	−0.89
$[M + 131]^+$	0.64	0.09	−4.4	0.7	0.89
$[M + 131]^+ + [M + 111]^+ + [M + 91]^+ + [M + 49]^+$	0.78	0.10	−5.5	0.7	0.91

[a] Ion counts have been normalized by dividing by the summed intensity of all the major ions observed.
[b] These results are for the PAHs listed in Table 5 and 6.
[c] Unitless because relative ion counts are unitless.

ion chromatograms causes the phenanthrenes (**1b** and methyl-**1b**, positions 1 and 3) to plot positive and the anthracenes (**1a** and methyl-**1a**, positions 2 and 4) to plot negatively (Fig. 7). The other signals eluting beyond position 4 can be assigned accordingly to other **1a** (negative deflection) and **1b** (positive deflection) monomethyl analogues.

5. Conclusion

Individual ions mass selected from FC43 can be used as reagents in ion/molecule reactions for the differentiation of PAH isomers in a quadrupole ion trap mass spectrometer. In particular, CF_3^+ and $C_3F_5^+$ ions were analytically useful for the analysis of a

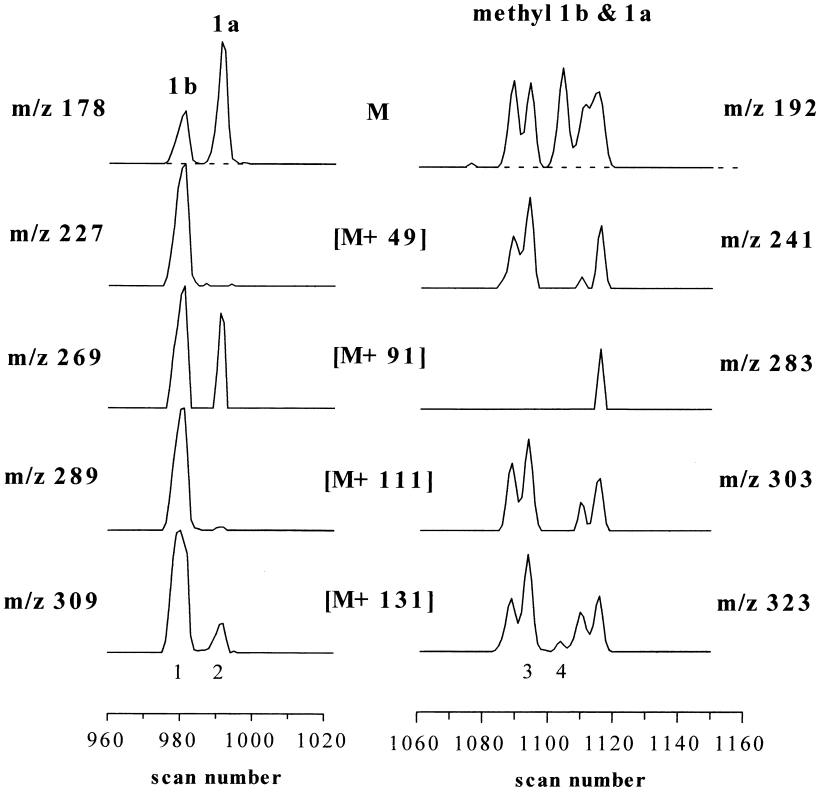

Fig. 5. Extracted M, [M + 49], [M + 91], [M + 111], and [M + 131] ion chromatograms for (left) phenanthrene (**1b**) and anthracene (**1a**) and (right) monomethyl phenanthrenes and anthracenes (multiple peaks are due to presence of mono methyl positional isomers).

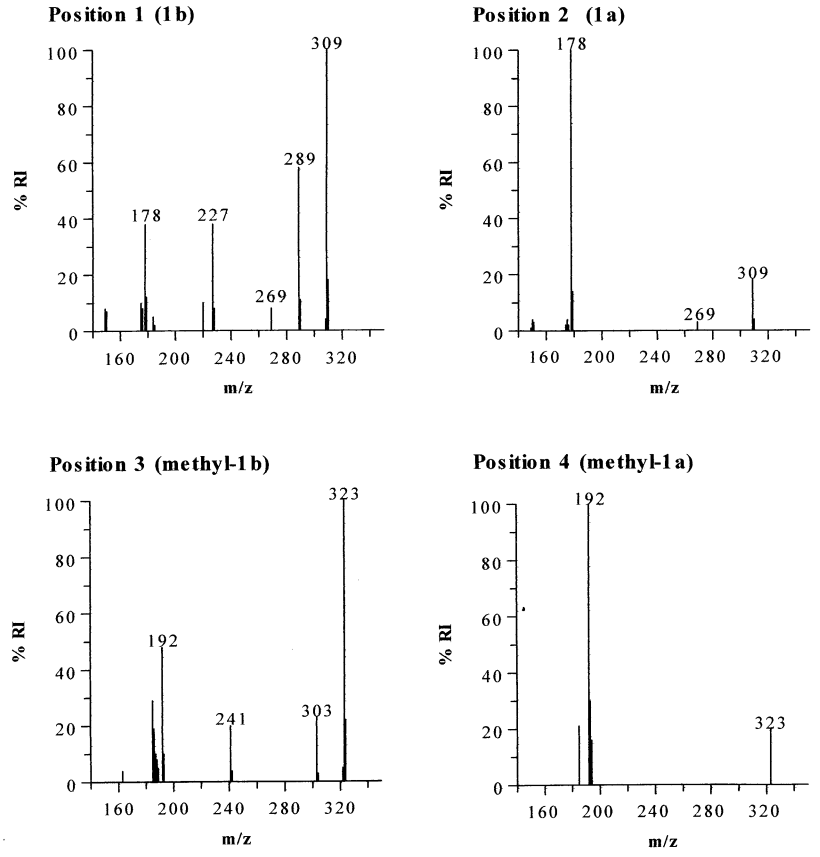

Fig. 6. Mass spectral data extracted at selected positions in the ion chromatograms illustrated in Fig. 5.

variety of PAHs isomers. Formation of ion/molecule reaction products appears to be strongly correlated to the IE of the PAH compounds. The highest abundance of reaction products occurred between PAHs with high IE such as **1b** (IE = 7.9 eV), and reagent ions with lower IE, such as $C_3F_5^+$ (IE $\leq$ 7.9 eV). Application of this technique to the analysis of PAHs in a contaminated sediment extract enabled differentiation of closely eluting methylated isomers of anthracene and phenanthrene. Thus FC43 could prove to be more useful than just as a mass calibration standard. Other compounds, such as perfluorokerosene (PFK), also used frequently as mass calibrant produce the same two ion species. In consideration of the data presented here, one should also be aware that during mass spectrometric analyses of compounds with structural features similar to PAHs, leakage from the reference inlet system could produce artifacts that would not be eliminated by routine background subtraction.

Acknowledgements

The authors thank Varian Canada for the extended loan of the MS/MS and CI features of the Saturn 4D ion trap. The authors acknowledge financial support from Dr. K. Reimer of the Royal Canadian Military College Environmental Sciences Group, from the Department of Indian and Northern Development (DIAND), and the National Science and Engineering Research Council of Canada (NSERC).

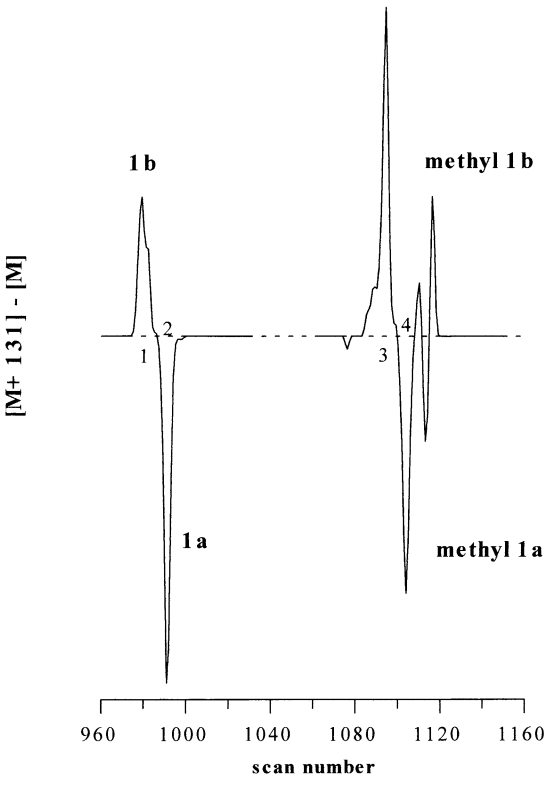

Fig. 7. Transformation ion chromatograms for (left) phenanthrene (**1b**) and anthracene (**1a**) and (right) mono methyl-**1a**/**1b** isomers.

References

[1] NRCC Publication No. 18981, Polycyclic Aromatic Hydrocarbons in the Aquatic Environment: Formation, Sources, Fate and Effects on Aquatic Systems, NRCC, Ottawa, 1983.
[2] R.G. Harvey, Polycyclic Aromatic Hydrocarbons: Chemistry and Carcinogenesis, Cambridge University Press, Cambridge, 1991.
[3] E.A. Stemmler, M.V. Buchanan, Rapid Commun. Mass Spectrom. 2 (184) 88.
[4] E.A. Stemmler, M.V. Buchanan, Org. Mass Spectrom. 24 (94) 89.
[5] E.A. Stemmler, M.V. Buchanan, Org. Mass Spectrom. 24 (705) 89.
[6] E.A. Stemmler, M.V. Buchanan, J. Mass Spectrom. 28 (953) 93.
[7] E.A. Stemmler, Int. J. Mass Spectrom. Ion Processes 142 (177) 95.
[8] P.G. Sim, C.M. Elson, Rapid Commun. Mass Spectrom. 2 (137) 88.
[9] C.M. Elson, P.G. Sim, Rapid Commun. Mass Spectrom. 4 (37) 90.
[10] E.P. Burrows, J. Mass Spectrom. 30 (312) 95.
[11] A. Milliet, M.F. Renou-Gonnord, K. Pointet, Anal. Environ. Chem. 322 (347) 96.
[12] K. Pointet, A. Milliet, M.F. Renou-Gonnord, P. Fleurat-Lessard, Eur. Mass Spectrom. 3 (281) 97.
[13] A.A. Mosi, Analysis of Polycyclic Aromatic Hydrocarbons by Chemical Ionization and Ion Trap Mass Spectrometry, University of British Columbia, Vancouver, 1998.
[14] S. Catinella, P. Traldi, X. Jiang, F.A. Londry, R.J.S. Morrison, R.E. March, S. Gregoire, J. Mathurin, J. Tabet, Rapid Commun. Mass Spectrom. 9 (1302) 95.
[15] A.A. Mosi, K.J. Reimer, G.K. Eigendorf, Talanta 44 (985) 97.
[16] A.A. Mosi, W.R. Cullen, G.K. Eigendorf, J. Mass Spectrom. 32 (864) 97.
[17] A.A. Mosi, W.R. Cullen, G.K. Eigendorf, J. Mass Spectrom. 33 (250) 98.
[18] M. Tsuji, M. Aizawa, Y. Nishimura, Chem. Lett. (211) 95.
[19] M. Tsuji, M. Aizawa, H. Ujita, Y. Nishimura, Y. Bull. Chem. Soc. Jap. 68 (2385) 95.
[20] M. Tsuji, M. Aizawa, Y. Nishimura, Y. J. Mass Spectrom. Soc. Jpn. 43 (109) 95.
[21] M. Tsuji, M. Aizawa, Y. Nishimura, Bull. Chem. Soc. Jpn. 69 (147) 96.
[22] D.R. Lide (Ed.), CRC Handbook of Chemistry and Physics, 73rd ed., CRC, Boca Raton, 1992.
[23] S.G. Lias, J.E. Bartmess, J.F. Liebman, J.L. Holmes, R.D. Levin, W.G. Mallard, J. Phys. Chem. Ref. Data 17 (1998) (suppl).